

Setting the scale for the Lüscher-Weisz action

**Christof Gattringer[†], Roland Hoffmann
and Stefan Schaefer**

Institut für Theoretische Physik
Universität Regensburg
93040 Regensburg, Germany

Abstract

We study the quark-antiquark potential of quenched SU(3) lattice gauge theory with the Lüscher-Weisz action. After blocking the gauge fields with the recently proposed hypercubic transformation we compute the Sommer parameter, extract the lattice spacing a and set the scale at 6 different values of the gauge coupling in a range from $a = 0.084$ fm to 0.136 fm.

PACS: 11.15.Ha

Key words: Lattice gauge theory, static potential, improvement

[†] Supported by the Austrian Academy of Sciences (APART 654).

Recently a noticeable revival of the interest in improved gauge actions took place. It was observed that improved gauge actions make the numerical problems less severe when implementing chiral fermions. The underlying mechanism for the numerical improvement is a suppression of ultraviolet fluctuations of the gauge field. An example is the use of the Iwasaki and other improved gauge actions for domain wall fermions [1] and also using the perfect gauge action [2] is an integral part of constructing the fixed point Dirac operator [3]. Recently a systematic expansion of a solution of the Ginsparg-Wilson equation [4], the so-called chirally improved fermion, was proposed and implemented [5]. Also there it was found that using the improved gauge action is numerically advantageous for the Dirac operator. In particular the Lüscher-Weisz action [6] with coefficients from tadpole improved perturbation theory [7, 8] was used. Subsequently the instanton content of the QCD vacuum was studied for the Lüscher-Weisz action in [9].

In this letter we report on our results for the static potential and the lattice scale for the Lüscher-Weisz action in order to make the use of this action easily accessible to the community. We furthermore test the recently proposed method of hypercubic blocking [10] which was found [10, 11] to improve the statistical accuracy in the determination of the static potential by an order of magnitude. We analyze quenched ensembles at 6 different values of the gauge coupling and compute the Sommer parameter [12, 13] and the lattice spacing a . This results in a precise determination of the lattice scale in a range between $a = 0.084$ fm to $a = 0.136$ fm and using a fit to our data even beyond this interval. Together with our results for the secondary couplings β_2 and β_3 this letter provides all ingredients necessary for using the Lüscher-Weisz action at typical lattice spacings of state of the art simulations.

In addition to the plaquette term of the Wilson gauge action, the Lüscher-Weisz action includes a sum over all 2×1 rectangles and a sum over all parallelograms, i.e. all possible closed loops of length 6 along the edges of all 3-cubes. Explicitly the action reads

$$\begin{aligned}
S[U] = & \beta_1 \sum_{pl} \frac{1}{3} \text{Re Tr} [1 - U_{pl}] + \beta_2 \sum_{rt} \frac{1}{3} \text{Re Tr} [1 - U_{rt}] \\
& + \beta_3 \sum_{pg} \frac{1}{3} \text{Re Tr} [1 - U_{pg}] ,
\end{aligned} \tag{1}$$

where β_1 is the principal parameter while β_2 and β_3 can be computed [7]

from β_1 using tadpole improved perturbation theory [8],

$$\beta_2 = -\frac{\beta_1}{20 u_0^2} [1 + 0.4805 \alpha] , \quad \beta_3 = -\frac{\beta_1}{u_0^2} 0.03325 \alpha , \quad (2)$$

with

$$u_0 = \left(\frac{1}{3} \text{Re Tr} \langle U_{pl} \rangle \right)^{1/4} , \quad \alpha = -\frac{\ln \left(\frac{1}{3} \text{Re Tr} \langle U_{pl} \rangle \right)}{3.06839} . \quad (3)$$

The couplings β_2, β_3 are determined self-consistently from u_0 and α for a given β_1 . In Table 1 we list the values of the β_i used for our ensembles and our results for the expectation value of the plaquette $u_0^4 = \text{Re Tr} \langle U_{pl} \rangle / 3$. The sample size at each value of β_1 is 200 configurations on 16^4 lattices. The update was done with a mix of Metropolis and over-relaxation sweeps.

β_1	8.00	8.10	8.20	8.30	8.45	8.60
u_0^4	0.62107(3)	0.62894(3)	0.63599(3)	0.64252(3)	0.65176(3)	0.66018(3)
β_2	-0.54574	-0.54745	-0.54998	-0.55332	-0.55773	-0.56345
β_3	-0.05252	-0.05120	-0.05020	-0.04953	-0.04829	-0.04755

Table 1: Parameters for the Lüscher-Weisz action. We list the values of the β_i and the expectation value of the plaquette $u_0^4 = \text{Re Tr} \langle U_{pl} \rangle / 3$.

Before measuring the potential we applied the hypercubic blocking transformation proposed in [10]. Hypercubic blocking mixes only gauge links from the hypercubes attached to the target link and has less impact on the short distance properties of the gauge fields than previously used smearing methods. The hypercubic blocking transformation proceeds in three steps [10]:

$$\begin{aligned} \bar{V}_{i,\mu;\nu\rho} &= \mathcal{P}_{SU(3)} \left[(1 - \alpha_3) U_{i,\mu} + \frac{\alpha_3}{2} \sum_{\pm\eta \neq \rho, \nu, \mu} U_{i,\eta} U_{i+\hat{\eta},\mu} U_{i+\hat{\mu},\eta}^\dagger \right] , \\ \tilde{V}_{i,\mu;\nu} &= \mathcal{P}_{SU(3)} \left[(1 - \alpha_2) U_{i,\mu} + \frac{\alpha_2}{4} \sum_{\pm\rho \neq \nu, \mu} \bar{V}_{i,\rho;\nu\mu} \bar{V}_{i+\hat{\rho},\mu;\rho\nu} \bar{V}_{i+\hat{\mu},\rho;\nu\mu}^\dagger \right] , \\ V_{i,\mu} &= \mathcal{P}_{SU(3)} \left[(1 - \alpha_1) U_{i,\mu} + \frac{\alpha_1}{6} \sum_{\pm\nu \neq \mu} \tilde{V}_{i,\nu;\mu} \tilde{V}_{i+\hat{\nu},\mu;\nu} \tilde{V}_{i+\hat{\mu},\nu;\mu}^\dagger \right] . \end{aligned} \quad (4)$$

In the first step intermediate fields $\bar{V}_{i,\mu;\nu\rho}$ are created from the thin-link variables $U_{i,\mu}$ (indices i run over all sites of the lattice and μ, ν, ρ and η over

the four directions). In the second step the intermediate fields $\bar{V}_{i,\mu;\nu\rho}$ are blocked into a second set of intermediate fields $\tilde{V}_{i,\mu;\nu}$ which in the third step are transformed into the final fields $V_{i,\mu}$. The restrictions on the indices μ, ν and ρ implemented in the sums in Eqs. (4) ensure that $V_{i,\mu}$ contains only contributions from the hypercubes attached to the link (i, μ) . By $\mathcal{P}_{SU(3)}$ we denote the projection of the sums back to elements of $SU(3)$. The parameters α_1, α_2 and α_3 determine the admixture of staples in each step of the blocking process. These parameters were optimized [10] to minimize the fluctuations of the plaquette. Their values are given by $\alpha_1 = 0.75, \alpha_2 = 0.6$ and $\alpha_3 = 0.3$.

We measured the static potential on the smeared configurations using planar Wilson loops $W(r, t)$ of size $r \times t$ with both t and r ranging from 1 to 10. We fitted the expectation values of the Wilson loops to a sum of two exponentials $c_1 \exp(-V(r)t) + c_2 \exp(-E't)$ in a range of $t = 2, 3 \dots 9$. The second exponential takes into account the contribution from excited states $E' > V(r)$ and from the first term we directly obtain the potential $V(r)$ for two static sources at distance r . As a cross check we also computed for some of the ensembles the potential for the raw, unblocked configurations. We find that the results are compatible within error bars but the statistical fluctuations, in particular at larger values of r and t , are much more severe for the raw configurations.

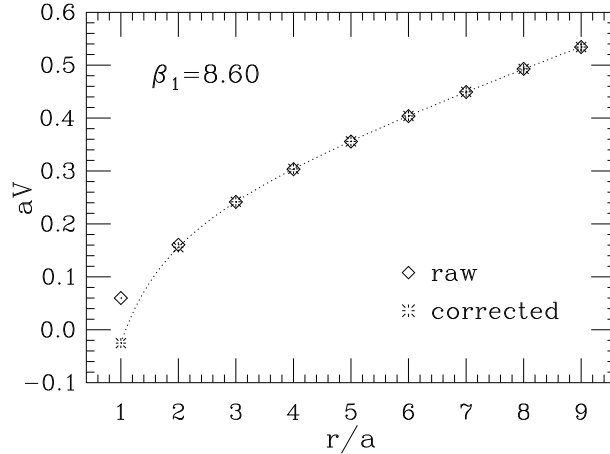


Figure 1: The static potential for the $\beta_1 = 8.60$ ensemble. The diamonds represent the raw data from the two parameter fit on the Wilson loops and the bursts are the values corrected for the short distance effect of the hypercubic blocking. The full curve is the parameterization (5).

In Fig. 1 we show our results for the static potential for the $\beta_1 = 8.60$ ensemble. The smooth curve is the standard infrared parameterization for the continuum potential,

$$V(r) = C - A/r + \sigma r, \quad (5)$$

with constants C, A and σ . The diamonds are the values for the potential obtained from the Wilson loops. The error bars are smaller than the symbols. For small distances, one finds a noticeable deviation from the Coulomb behavior $-A/r$. This deviation is an effect of the hypercubic blocking. However, this effect can be computed perturbatively and the obtained deviation from the Coulomb potential is used to introduce a fourth fit parameter in the potential fit [11]. Subtracting this perturbative part gives the corrected data which we represent by bursts. From the parameters A and σ we computed the Sommer parameter r_0 [13] in lattice units a and assuming $r_0 = 0.5$ fm we extracted the lattice spacing a . We give the results for the lattice spacing and the Sommer parameter in Table 2.

β_1	8.00	8.10	8.20	8.30	8.45	8.60
r_0/a	3.688(37)	4.015(34)	4.362(41)	4.741(49)	5.289(66)	5.967(70)
a [fm]	0.136(1)	0.125(1)	0.115(1)	0.105(1)	0.095(1)	0.084(1)

Table 2: Results for the Sommer parameter r_0 in lattice units and the corresponding values for the lattice spacing a when r_0 is assumed as $r_0 = 0.5$ fm.

In order to make the Sommer parameter and the lattice spacing available also for other values of β_1 we fit our data to a functional form based on the β -function as proposed in [13]. We find

$$\ln(r_0/a) = 1.55354 + 0.79840(\beta_1 - 8.3) - 0.09533(\beta_1 - 8.3)^2. \quad (6)$$

In Fig. 2 we compare our numerical data for r_0/a and a (again assuming $r_0 = 0.5$ fm) to the curve (6). It is obvious that the data are well described by our parameterization. Furthermore when extending the plot range to values of β_1 as small as $\beta_1 = 6.8$ we find that our results are in good agreement with the data computed for very coarse lattices in [7], i.e. $a = 0.24$ fm at $\beta_1 = 7.4$, $a = 0.33$ fm at $\beta_1 = 7.1$ and $a = 0.40$ fm at $\beta_1 = 6.8$.

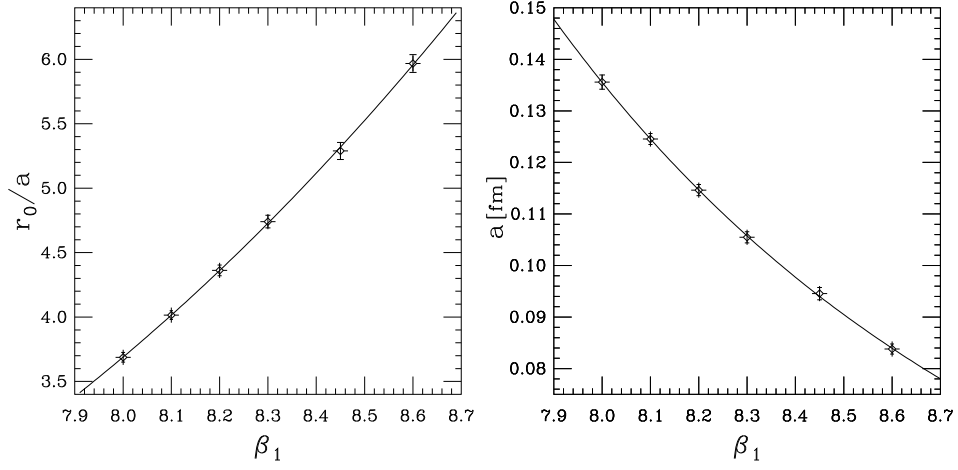


Figure 2: Results for the Sommer parameter in lattice units (left-hand side plot) and the lattice spacing in fermi (right-hand side plot) as a function of β_1 . The full curves are the interpolations of the data with the function (6).

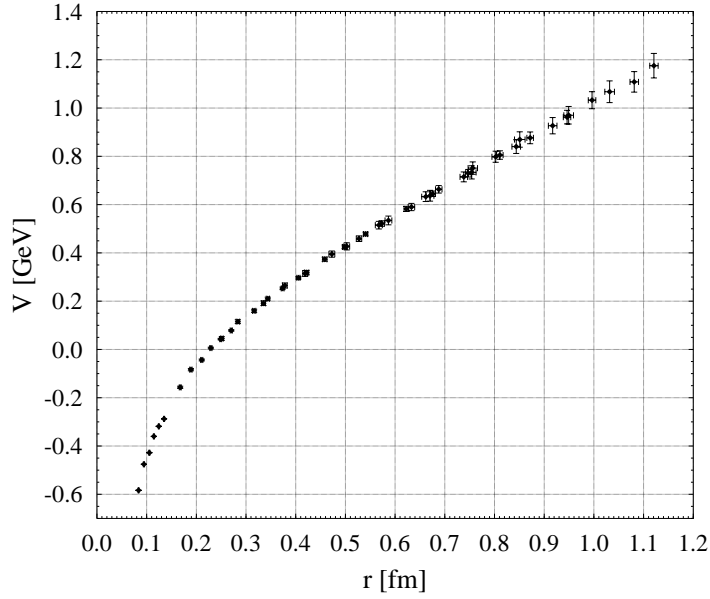


Figure 3: Superposition of the potentials for all values of β_1 . The irrelevant constant C in Formula (5) is set to zero.

Finally in Fig. 3 we show a common plot of our results for the static potential at all values of β_1 we analyzed. We set the irrelevant overall constant C to zero for all β_1 . It is obvious that the data from different lattice spacings are in perfect agreement and the discretization errors are hardly noticeable for the Lüscher-Weisz action.

Acknowledgements: We would like to thank Meinulf Göckeler, Anna Hasenfratz, Francesco Knechtli, Paul Rakow and Andreas Schäfer for interesting discussions.

References

- [1] K. Orginos, hep-lat/0110074; L. I. Wu, Nucl. Phys. Proc. Suppl. 83 (2000) 224, A. Ali Khan *et al.*, Nucl. Phys. Proc. Suppl. 83 (2000) 591.
- [2] T. DeGrand, A. Hasenfratz, P. Hasenfratz and F. Niedermayer, Nucl. Phys. B 454 (1995) 587, Nucl. Phys. B 454 (1995) 615 and Phys. Lett. B 365 (1996) 233.
- [3] P. Hasenfratz, Nucl. Phys. B (Proc. Suppl.) 63 (1998) 53; and Nucl. Phys. B 525 (1998) 401; P. Hasenfratz, S. Hauswirth, K. Holland, T. Jörg, F. Niedermayer and U. Wenger, Nucl. Phys. Proc. Suppl. 94 (2001) 627 and hep-lat/0109004.
- [4] P.H. Ginsparg and K.G. Wilson, Phys. Rev. D 25 (1982) 2649.
- [5] C. Gattringer, Phys. Rev. D 63 (2001) 114501; C. Gattringer and I. Hip, Phys. Lett. B 480 (2000) 112; C. Gattringer, I. Hip and C.B. Lang, Nucl. Phys. B597 (2001) 451.
- [6] M. Lüscher and P. Weisz, Commun. Math. Phys. 97 (1985) 59; Erratum: 98 (1985) 433; G. Curci, P. Menotti and G. Paffuti, Phys. Lett. B 130 (1983) 205, Erratum: B 135 (1984) 516.
- [7] M. Alford, W. Dimm, G.P. Lepage, G. Hockney and P.B. Mackenzie, Phys. Lett. B 361 (1995) 87.
- [8] G.P. Lepage and P.B. Mackenzie, Phys. Rev. D 48 (1993) 2250.
- [9] C. Gattringer, M. Göckeler, P.E.L. Rakow, S. Schaefer and A. Schäfer, Nucl. Phys. B 617 (2001) 101 and Nucl. Phys. B 618 (2001) 205.

- [10] A. Hasenfratz and F. Knechtli, Phys. Rev. D 64 (2001) 034504.
- [11] A. Hasenfratz, R. Hoffmann and F. Knechtli, hep-lat/0110168.
- [12] R. Sommer, Nucl. Phys. B 411 (1994) 839.
- [13] M. Guagnelli, R. Sommer and H. Wittig, Nucl. Phys. B 535 (1998) 389.